

Electronic supplementary information (ESI)

***In situ* synthesis of reduced graphene oxide/polyethyleneimine
composite and its gas barrier properties**

Hongyu Liu^{a,b}, Tapas Kuila^a, Nam Hoon Kim^c, Bon-Cheol Ku^d, Joong Hee Lee^{a,c,e*}

^aDepartment of BIN Fusion Technology, Chonbuk National University, Jeonju,
Jeonbuk, 561-756, Republic of Korea

^bDepartment of Chemical Engineering & Pharmaceutics, Henan University of Science
& Technology, Luoyang, China

^cDepartment of Hydrogen and Fuel Cell Engineering, Chonbuk National University,
Jeonju, Jeonbuk, 561-756, Republic of Korea

^dInstitute of Advanced Composites Materials, Korea Institute of Science and
Technology Eunha-ri san 101, Bondong-eup, Wanju-gun,
Jeollabuk-do, 565-902, Korea

^eBIN Fusion Research Center, Department of Polymer & Nano Engineering, Chonbuk
National University, Jeonju, Jeonbuk, 561-756, Republic of Korea

*Corresponding author. Tel.: 82-63-270-2342, Fax: 82-63-270-2341,

E-mail address: jhl@jbnu.ac.kr (Joong Hee Lee)

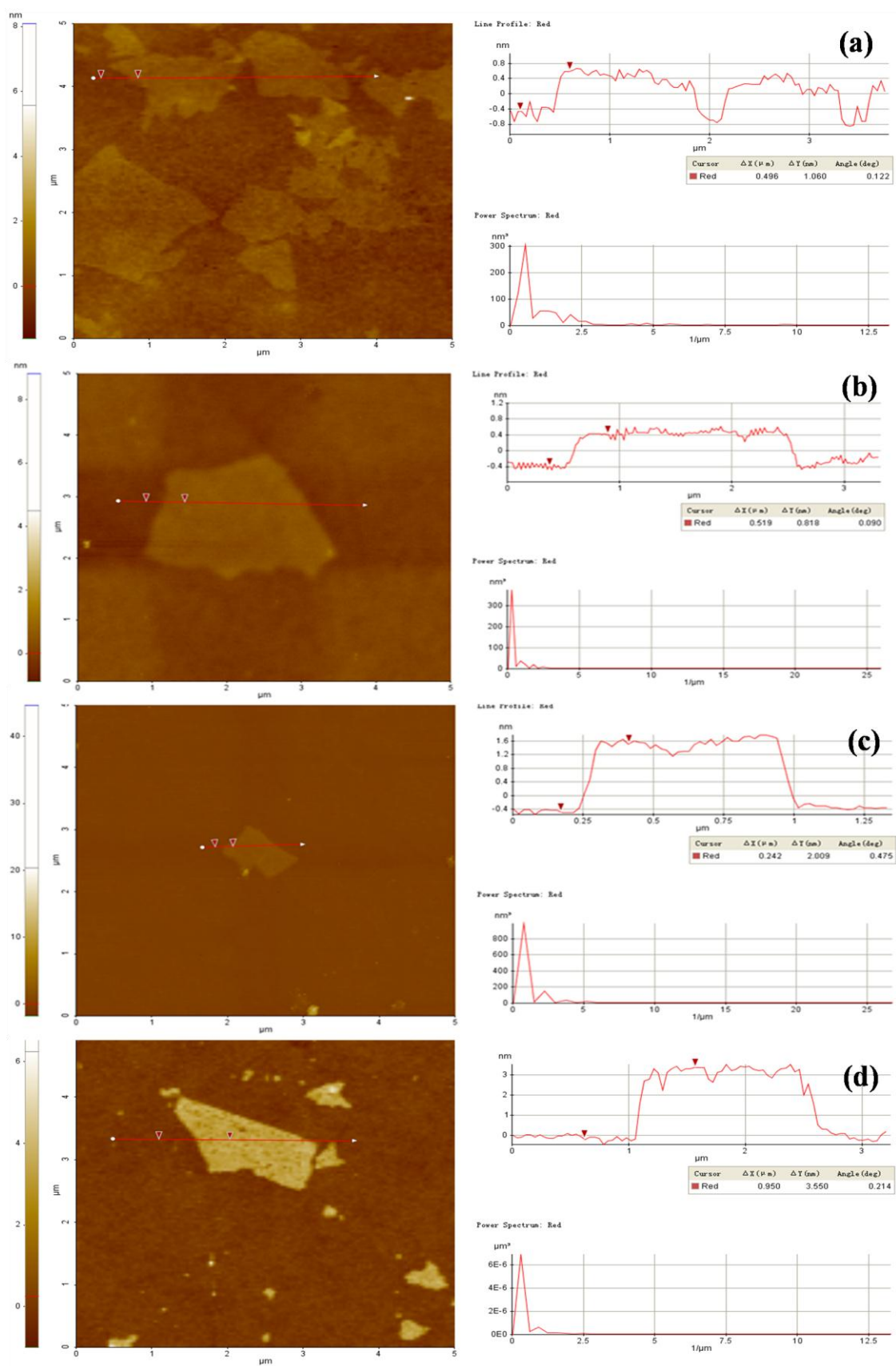


Fig. S1 AFM images of (a) GO, (b) PEI-0.02-RGO, (c) PEI-1-RGO and (d)

PEI-3-RGO.

The single layer GO was produced from graphite oxide *via* 30 min sonication at room temperature. The successful exfoliation of GO was confirmed by atomic force microscopy (AFM). As shown in Fig. S1(a), single layer GO is obtained with the thickness of about 1 nm and the size distribution of the sheets is wide. This is consistent with the previous work.¹ This wide size distribution is expected to increase the gas barrier properties of the film.² However, the thickness of the PEI-0.02-RGO is around 0.82 nm, suggesting the successful removal of the oxygen containing groups from the GO sheets, similar to previous reports.^{3,4} On the other hand, the AFM images of PEI-1-RGO and PEI-3-RGO exhibit the thickness of around 2.0 and 3.6 nm, respectively, demonstrating the introduction of PEI onto the RGO sheets, which is a good agreement with previous work.⁵

The electrical conductivities of the specimens are of great importance to evaluate how the π conjugated system is restored within the RGO sheets. The conductivities of the resultant RGO as well as pristine GO were measured to elucidate the reduction of GO to RGO and the attachment of PEI onto the surface of RGO. As we can see in Table S1, the original GO is an insulator (0.002 S m^{-1}). When a small PEI:GO ratio (PEI-0.02-RGO) is employed, the conductivity of the resultant RGO is greatly improved to 492 S m^{-1} . This value even outperforms than that of the hydrazine reduced equivalent.¹ However, when the PEI content is continuously increased, the electrical conductivities of the resultant RGO are dramatically decreased. This is due to the nonconductive PEI chemically attached to the surface of the RGO, forming PEI

surface modified RGO. As to PEI-5-RGO, the powder obtained by mortar and pestle, however, cannot be made into a pellet so we cannot perform the conductivity measurement with the four-probe method. Note that when more PEI is used (PEI-3-RGO), the conductivity of the resultant PEI-RGO is 0.783 S m^{-1} , 2 orders of magnitude higher than that of pristine GO, showing the reduction of GO. However, in comparison to the value of the RGO with low PEI content, the decrease of conductivity illuminates the successful introduction of PEI onto the RGO surface. This tunable electrical conductivity endows the PEI-RGO with potential applications for electronics among other things. For our purposes, we would like to assemble the PEI-RGO sheets into a layered thin film for improved barrier property where the PEI acts as the polymer matrix.

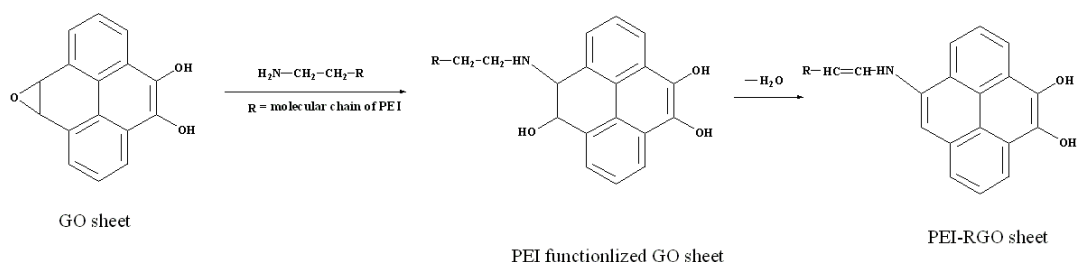
Table S1. Electrical conductivities of the neat GO and RGO

Reducing agent	Sample name	Electrical conductivity S m^{-1}	Reference
PEI	PEI-0.02-RGO	492	Present study
PEI	PEI-0.25-RGO	125	Present study
PEI	PEI-0.5-RGO	28	Present study
PEI	PEI-1-RGO	0.783	Present study
PEI	PEI-3-RGO	0.159	Present study
-----	GO	0.002	Present study
Hydrazine	-----	200	1
NaBH_4	-----	45	6
L-ascorbic acid	-----	800	7
<i>p</i> -phenylene diamine	-----	210	8
Tea	-----	53	9
Yeast	-----	43	10

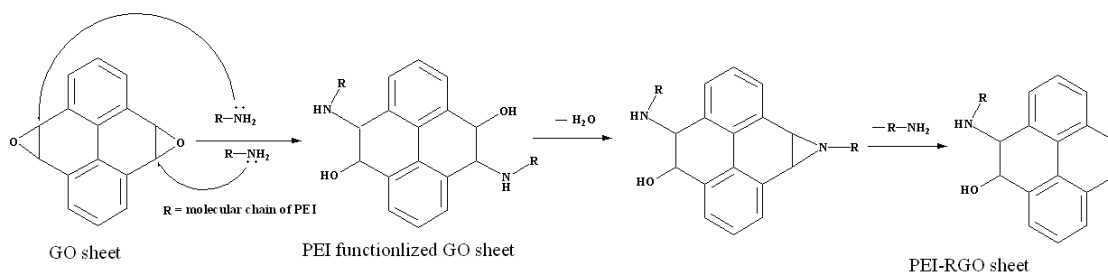
Table S2. Atomic concentrations of GO and PEI-1-RGO.

Sample	Carbon (at%)	Oxygen (at%)	Nitrogen (at%)	C/O ratio
GO	67.3	32.7	0.0	2.1
PEI-1-RGO	77.8	13.9	8.3	5.6

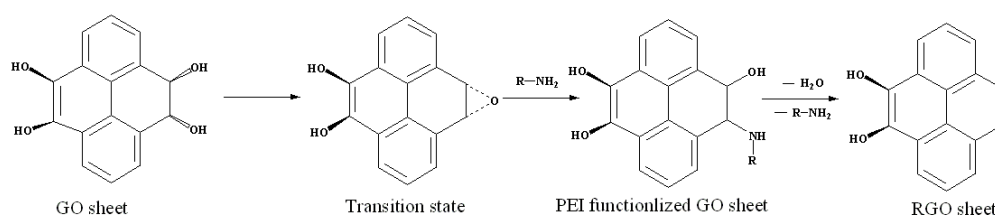
Mechanism 1



Mechanism 2



Mechanism 3



Mechanism 4

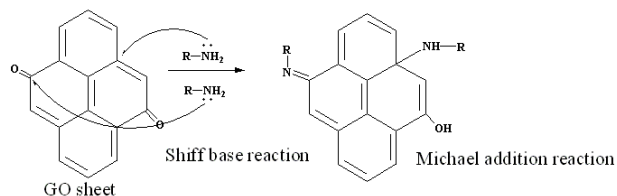


Fig. S2 Mechanisms of reduction and surface modification of GO to PEI-RGO.

References

1. S. Stankovich, D. A. Dikin, R. D. Piner, K. A. Kohlhaas, A. Kleinhammes, Y. Y. Jia, Y. Wu, S. T. Nguyen and R. S. Ruoff, *Carbon*, 2007, **45**, 1558-1565.
2. N. K. Lape, E. E. Nuxoll and E. L. Cussler, *J. Membrane Sci.*, 2004, **236**, 29-37.
3. X. G. Mei and J. Y. O, *Carbon*, 2011, **49**, 5389-5397.
4. W. Chen, L. Yan and P. R. Bangal, *J. Phys. Chem. C*, 2010, **114**, 19885-19890.
5. B. Zhang, Y. Zhang, C. Peng, M. Yu, L. Li, B. Deng, P. Hu, C. Fan, J. Li and Q. Huang, *Nanoscale*, 2012, **4**, 1742-1748.
6. H. J. Shin, K. K. Kim, A. Benayad, S. M. Yoon, H. K. Park, I. S. Jung, M. H. Jin, H. K. Jeong, J. M. Kim, J. Y. Choi and Y. H. Lee, *Adv. Funct. Mater.*, 2009, **19**, 1987-1992.
7. J. L. Zhang, H. J. Yang, G. X. Shen, P. Cheng, J. Y. Zhang and S. W. Guo, *Chem. Commun.*, 2010, **46**, 1112-1114.
8. H. L. Ma, H. B. Zhang, Q. H. Hu, W. J. Li, Z. G. Jiang, Z. Z. Yu and A. Dasari, *ACS Appl. Mater. Interfaces*, 2012, **4**, 1948-1953.
9. Y. Wang, Z. X. Shi and J. Yin, *ACS Appl. Mater. Interfaces*, 2011, **3**, 1127-1133.
10. P. Khanra, T. Kuila, N. H. Kim, S. H. Bae, D.S. Yu and J. H. Lee, *Chemical Engineering Journal*, 2012, **183**, 526-533.